HHS Public Access

Author manuscript

Cancer Cell. Author manuscript; available in PMC 2017 June 13.

Published in final edited form as:

Cancer Cell. 2016 June 13; 29(6): 889–904. doi:10.1016/j.ccell.2016.04.015.

ARF6 is an actionable node that orchestrates oncogenic GNAQ signaling in uveal melanoma

Jae Hyuk Yoo[1,2,16], **Dallas S. Shi**[1,3,16], **Allie H. Grossmann**[1,4,5,16], **Lise K. Sorensen**[1], **ZongZhong Tong**[6,7], **Tara M. Mleynek**[1], **Aaron Rogers**[4], **Weiquan Zhu**[1], **Jackson R. Richards**[1,2], **Jacob M. Winter**[1], **Jie Zhu**[8], **Christine Dunn**[6], **Ashok Bajji**[6,9], **Mark Shenderovich**[6,10], **Alan L. Mueller**[6], **Scott E. Woodman**[11], **J. William Harbour**[12], **Kirk R. Thomas**[1,13], **Shannon J. Odelberg**[1,14], **Kirill Ostanin**[6,*], and **Dean Y. Li**[1,2,3,5,7,14,15,*]

[1]Department of Medicine, Program in Molecular Medicine, University of Utah, Salt Lake City, UT, 84112, USA

[2]Department of Oncological Sciences, University of Utah, Salt Lake City, UT 84112, USA

[3]Department of Human Genetics, University of Utah, Salt Lake City, UT 84112, USA

[4]Department of Pathology, University of Utah, Salt Lake City, UT 84112, USA

[5]ARUP Laboratories, University of Utah, Salt Lake City, UT 84112, USA

[6]Navigen Inc., Salt Lake City, UT 84108, USA

[7]Sichuan Provincial Key Laboratory for Human Disease Gene Study, Sichuan Provincial People's Hospital, Chinese Academy of Sciences, Chengdu, China

[8]Department of Ophthalmology and Shiley Eye Institute, University of California, San Diego, La Jolla, CA 92093

[9]VioGen Biosciences LLC, Salt Lake City, Utah, 84119, USA

[10]Mol3D Research LLC, Salt Lake City, Utah, 84124, USA

[*]Corresponding Authors: Dean Y. Li, Building 533 Room 4220, 15 North 2030 East, Salt Lake City, UT 84112, USA Phone: 801-585-5505; Fax: 801-585-0701; dean.li@u2m2.utah.edu, Kirill Ostanin, Navigen Inc., 383 Colorow Drive, Salt Lake City, UT 84108, USA Phone: 801-587-1456; kostanin@nvgn.com.

[16]These authors contributed equally to the work

SUPPLEMENTAL INFORMATION

Supplemental Information includes seven figures, three tables, and Supplemental Experimental Procedures.

AUTHOR CONTRIBUTIONS

J.H.Y., K.O., and D.Y.L. were responsible for project. J.H.Y., K.O., and D.Y.L. were responsible for conceptualization, experimental design, data analysis, and manuscript preparation. J.H.Y. primarily performed and collected data for *in vitro* experiments. D.S.S primarily performed and collected data for *in vivo* experiments. A.H.G. provided histology and pathology expertise. L.K.S. performed immunocytofluorescent staining. Z.T. and A.R. constructed several plasmids. T.M.M. performed immunocytofluorescent staining and helped prepare the figures. W.Z., J.R.R., J.M.W., J.Z., and C.D. performed *in vitro/in vivo* experiments. A.B. was responsible for organic synthesis and Z.T., A.B., A.L.M., and K.O. were responsible for the drug screen. M.S. was responsible for computer analysis and modeling of the protein structure. S.E.W. provided human uveal melanoma cells. J.W.H. provided snap-frozen uveal melanoma tissues. K.R.T. provided critical review of the manuscript and experimental advice. S.J.O. performed *in vivo* experiments, analyzed data for *in vitro/in vivo* experiments, and helped with manuscript preparation. K.O. and D.Y.L. were responsible for obtaining funding for the project.

[11]Department of Melanoma Medical Oncology, Department of Systems Biology, University of Texas, MD Anderson Cancer Center, Houston, TX 77054, USA

[12]Ocular Oncology Service, Bascom Palmer Eye Institute and Sylvester Comprehensive Cancer Center, University of Miami Miller School of Medicine, Miami, FL 33136, USA

[13]Department of Medicine, Division of Hematology, University of Utah, Salt Lake City, UT, 84112, USA

[14]Department of Medicine, Division of Cardiology, University of Utah, Salt Lake City, UT, 84112, USA

[15]Department of Cardiology, VA Salt Lake City Health Care System, Salt Lake City, UT, 84112, USA

SUMMARY

Activating mutations in Gαq proteins, which form the a subunit of certain heterotrimeric G proteins, drive uveal melanoma oncogenesis by triggering multiple downstream signaling pathways, including PLC/PKC, Rho/Rac, and YAP. Here we show that the small GTPase ARF6 acts as a proximal node of oncogenic Gαq signaling to induce all of these downstream pathways as well as β-catenin signaling. ARF6 activates these diverse pathways through a common mechanism—the trafficking of GNAQ and β-catenin from the plasma membrane to cytoplasmic vesicles and the nucleus, respectively. Blocking ARF6 with a small molecule reduces uveal melanoma cell proliferation and tumorigenesis in a mouse model, confirming the functional relevance of this pathway and suggesting a therapeutic strategy for Gα-mediated diseases.

Graphical abstract

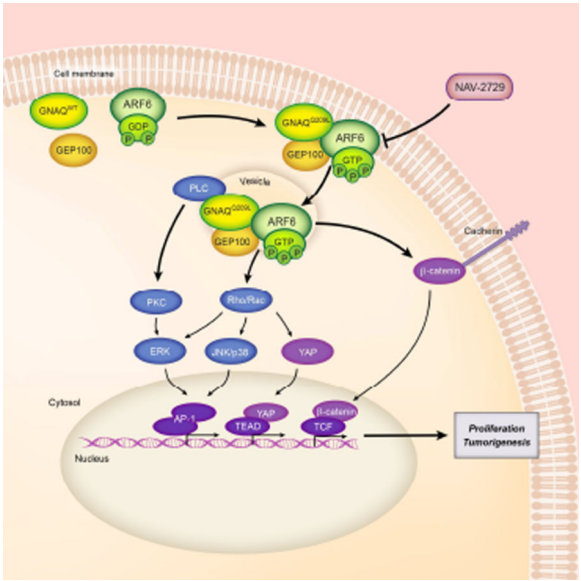

INTRODUCTION

Mutations that confer constitutive activity to G protein-coupled receptors (GPCRs) or Gα proteins have been identified in numerous diseases, including human cancers (Dorsam and Gutkind, 2007; Marinissen and Gutkind, 2001; O'Hayre et al., 2014; O'Hayre et al., 2013), McCune-Albright syndrome (Weinstein et al., 1991), and Sturge-Weber syndrome (Nakashima et al., 2014; Shirley et al., 2013). One such disease is uveal melanoma in which over 80% of tumors harbor an oncogenic activating mutation in either of two Gαq class (Gαq) proteins: GNAQ and GNA11 (Van Raamsdonk et al., 2009; Van Raamsdonk et al., 2010).

Uveal melanoma is the most common primary ocular malignancy, and there are no effective treatments for metastatic forms of this disease. The discovery of oncogenic *GNAQ* and *GNA11* mutations in uveal melanoma has led to the identification of multiple downstream signaling pathways that could be targeted for therapeutic purposes (Shoushtari and Carvajal, 2014). These signaling pathways include phospholipase C-b (PLC-β)/protein kinase C (PKC) and Rac1/RhoA, which lead to the activation of ERK, p38, JNK, and YAP and subsequent AP-1- and YAP/TEAD-mediated transcription (Feng et al., 2014; Khalili et al., 2012; Vaque et al., 2013; Wu et al., 2012b; Yu et al., 2014). However, it has been unclear how activating mutations in Gαq proteins exert their control over these divergent downstream pathways and whether activated Gαq proteins govern additional oncogenic pathways.

The small GTPase ADP-ribosylation factor 6 (ARF6) (Kahn and Gilman, 1984) is an attractive candidate for being an effector of Gαq signaling. ARF6 is activated by a variety of different ARF-guanine nucleotide exchange factors (ARF-GEFs), depending on the stimulating factor or cell type. Heterologous expression studies in HEK293T cells have suggested that activated Gαq proteins associate with various ARF-GEFs, which leads to the activation of ARF6 (Giguere et al., 2006; Laroche et al., 2007). Other studies have shown the crucial role ARF6 plays in invasion, metastasis, and proliferation of several different types of cancers (Grossmann et al., 2013; Hu et al., 2009; Hu et al., 2012; Li et al., 2009; Morishige et al., 2008; Muralidharan-Chari et al., 2009). ARF6 is a critical mediator of endocytosis and the recycling of multiple membrane receptors, including GPCRs and cadherin-catenin complexes (Chen et al., 2003; D'Souza-Schorey et al., 1995; Hunzicker-Dunn et al., 2002; Palacios et al., 2001). We recently demonstrated that in human cutaneous melanoma cells, WNT5A-stimulation of the GPCR FZD4 activates ARF6, which promotes the trafficking of β-catenin from its N-cadherin-bound membrane form to the nucleus where it stimulates TCF-mediated transcription (Grossmann et al., 2013).

In this study, we investigate the role of ARF6 as a mediator of all known oncogenic signaling pathways that are controlled by activating GNAQ mutations. The mechanism of ARF6 action is examined by determining whether it regulates GNAQ and β-catenin trafficking in uveal melanoma cells. We also assess the efficacy of targeting ARF6 for therapeutic purposes in a murine orthotopic xenograft model of human uveal melanoma. Finally, we seek to provide a mechanistic framework for studying other cancers harboring

activating Gα mutations and an alternative approach for identifying therapeutic targets for these cancers.

RESULTS

Oncogenic GNAQ promotes ARF6 activation to control the proliferation of uveal melanoma cells

We investigated whether ARF6 might also be important in cancers harboring somatic activating mutations of Gαq based on the reported role of ARF6 in several cancers (Grossmann et al., 2013; Hu et al., 2009; Hu et al., 2012; Li et al., 2009; Morishige et al., 2008; Muralidharan-Chari et al., 2009) and studies showing that Gαq proteins can activate or signal through ARF6 (Bose et al., 2001; Giguere et al., 2006; Laroche et al., 2007). We first examined ARF6 protein levels in human uveal melanomas that carried activating mutations in either *GNAQ* or *GNA11.* ARF6 protein levels were on average 1.7-fold higher in uveal melanomas than in normal choroid melanocytes isolated from eyes that were surgically removed due to uveal melanoma (Figure S1A). We next tested whether GNAQ in Mel92.1 and Mel202 uveal melanoma cells was required for ARF6 activation. Mel202 and Mel92.1 cells carry $GNAQ^{Q209L}$, the most common activating mutation in GNAQ (Griewank et al., 2012; Van Raamsdonk et al., 2009). The levels of ARF6-GTP were measured following *GNAQ* knockdown using two different siRNAs. Each knockdown reduced ARF-GTP levels by greater than 50% compared to a negative control siRNA that lacks homology to any known mammalian gene (Figure 1A). Consistent with these results, HEK293T cells transfected with vectors expressing $GNAQ^{Q209L}$ exhibited elevated levels of ARF6-GTP whereas those cells expressing wild-type GNAQ did not (Figure S1B). Knockdown of *GNAQ* in cultured uveal melanoma cells has been shown to inhibit cell growth (Van Raamsdonk et al., 2009). To determine if this inhibition is ARF6 dependent, we compared growth parameters between uveal melanoma cells transfected with siRNAs directed against *ARF6* or *GNAQ.* Knockdown of *ARF6* or *GNAQ* in both Mel92.1 and Mel202 cells caused similar reductions in cell proliferation and anchorage-independent colony growth (Figure 1B–1D). These results demonstrate a central role for ARF6 in oncogenic GNAQ-mediated cell proliferation.

To determine whether ARF6 activation can rescue reduced *GNAQ* expression, we expressed constitutively active ARF6 ($ARF6^{Q67L}$) in Mel202 cells while knocking down *GNAQ* expression. Both cell proliferation and anchorage-independent colony growth were partially rescued by constitutively active ARF6 when *GNAQ* expression was knocked down (Figure S1C–S1E), suggesting that the activation of ARF6 may serve to enhance oncogenic GNAQ signaling, not replace it. Constitutively active ARF6 may act through the residual GNAQ present following *GNAQ* knockdown to partially rescue the function of GNAQ.

GNAQ acts through ARF6 to orchestrate multiple downstream signaling pathways

Signaling pathways stimulated by oncogenic GNAQ include those mediated by PLC-PKC and Rac/Rho (Feng et al., 2014; Vaque et al., 2013; Wu et al., 2012a; Yu et al., 2014). Knockdown of either *ARF6* or *GNAQ* in uveal melanoma cells resulted in a significant reduction in PLC activity ranging from 24% to 80% inhibition when using a

phosphoinositide turnover assay (Figure 2A). Consistent with this reduction in PLC activity, the level of phosphorylated myristoylated alanine-rich C kinase substrate (p-MARCKS), a substrate of PKC, was decreased by *ARF6* knockdown (Figures 2B and S2A). Knockdown of *ARF6* or *GNAQ* also significantly reduced the levels of Rac1-GTP/RhoA-GTP and their downstream readouts, phosphorylated ERK, p38, JNK, and c-jun (Figures 2C–2E and S2B–S2G). The reduction of c-jun phosphorylation resulted in decreased AP-1 transcriptional activity (Figure 2F).

Oncogenic GNAQ enhances nuclear YAP activation through Rac1/RhoA, implicating YAP as a potential therapeutic target for uveal melanoma (Feng et al., 2014; Yu et al., 2014). Silencing *ARF6* or *GNAQ* inhibited by 60% the nuclear localization of YAP in uveal melanoma cells, as detected by immunocytofluorescence and subcellular fractionation/immunoblotting (Figures 2G, 2H, and S2H). mRNA levels of the YAP target genes *CYR61* and *CTGF* were also reduced in Mel92.1 and Mel202 cells in which ARF6 was knocked down (Figure 2I).

The finding that ARF6 is an effector of oncogenic GNAQ that activates multiple signaling pathways suggested that constitutively active ARF6 ($ARF6^{Q67L}$) would also activate these same pathways. Ectopic expression of $ARF6^{Q67L}$ or $GNAQ^{Q209L}$ in HEK293T cells induced the PLC-PKC and MAPK pathways, including the activation of ERK, p38, JNK, and c-jun and the increase in AP-1 transcriptional activity, YAP nuclear accumulation, and YAP-mediated transcription (Figure S2I–S2N). These results show that ARF6 is both necessary and sufficient, at least in cells expressing endogenous wild-type Gαq proteins, to mediate GNAQ activity and thus serves as a critical signaling node. However, based on the partial functional rescue that we achieved with constitutively active ARF6 following *GNAQ* knockdown in uveal melanoma cells and previous reports showing that Gαq proteins directly bind to and activate PLC-β1 (Berstein et al., 1992; Blank et al., 1991), we propose that activated ARF6 enhances GNAQ signaling and cannot entirely replace it.

$GNAQ^{Q209L}$-activated ARF6 induces β-catenin signaling by increasing β-catenin trafficking from the plasma membrane to the nucleus

Activating mutations in β-catenin are found in many human cancers (Clevers, 2006). Our previous work showed that in a model of cutaneous melanoma, WNT5A–activated ARF6 promotes the relocalization of β-catenin from the membrane to the nucleus to induce β-catenin-mediated transcription and cancer cell invasion and metastasis (Grossmann et al., 2013). We therefore examined whether the oncogenic GNAQ-activated ARF6 also increased the translocation of β-catenin from the membrane to the nucleus in uveal melanoma cells. Knocking down *GNAQ* or *ARF6* in uveal melanoma cells resulted in an increase in the membrane pool of β-catenin and a corresponding decrease in the cytosolic and nuclear pools, as shown by both immunocytofluorescence and subcellular fractionation analyses (Figure 3A and 3B). These treatments also significantly reduced luciferase activity in a 7TFP-mediated luciferase reporter assay (a measure of β-catenin-mediated transcription) (Figure 3C). Knockdown of *GNAQ* and *ARF6* did not alter total β-catenin protein levels (Figure S3A), suggesting that the mechanism that controls β-catenin intracellular localization by $GNAQ^{Q209L}$-activated ARF6 is independent of the mechanism of β-catenin

stabilization by WNTs. In HEK293T cells, ectopic expression of ARF6^{Q67L} or GNAQ^{Q209L} decreased the membrane pool of β-catenin and concomitantly increased the cytosolic and nuclear pools of β-catenin (Figure S3B). These same active forms of ARF6 and GNAQ also increased the activity of a β-catenin responsive luciferase reporter (Figure S3C). Together, these results show that an oncogenic Gαq protein induces β-catenin signaling and that it does so through the activation of its effector ARF6, which promotes the relocalization of β-catenin from the plasma membrane to the nucleus.

Other investigators have shown that ERK activation induces casein kinase-2 (CK2)-mediated phosphorylation of α-catenin, which destabilizes adherens junctions and releases β-catenin from cadherins (Ji et al., 2009; Pellon-Cardenas et al., 2013), and that this activation can be induced by ARF6 in epithelial cells (Pellon-Cardenas et al., 2013). To determine whether a similar mechanism drives β-catenin release in uveal melanoma cells, we knocked down *CK2α* (the catalytic subunit) and determined the intracellular location of β-catenin by subcellular fractionation. *CK2α* knockdown simultaneously increased β-catenin in the membrane fraction and decreased its localization to the cytoplasm and nucleus (Figure S3D), suggesting that a similar ERK-CK2-α-catenin mechanism may control β-catenin release from cadherins in uveal melanoma cells.

β-catenin signaling can increase cell proliferation in some cancer cells (Clevers, 2006; Reya and Clevers, 2005). To determine whether β-catenin signaling in uveal melanoma cells influences cell proliferation, we exposed Mel92.1 and Mel202 cells to two different inhibitors of β-catenin signaling, XAV-939 and IWR-1-endo (Chen et al., 2009; Huang et al., 2009). After 72 hours of treatment, both XAV939 and IWR-1-endo inhibited cell proliferation in a concentration-dependent manner with a GI_{50} (50% growth inhibition) of around 3 μM and 10 μM, respectively, in both cell lines (Figure S3E). These results suggest that GNAQ^{Q209L}-ARF6-mediated β-catenin signaling plays a role in uveal melanoma cell proliferation.

Oncogenic GNAQ forms a complex with GEP100 to activate ARF6

We next sought to identify the ARF-GEF responsible for oncogenic GNAQ-mediated ARF6 activation. ARNO and GEP100 are known ARF6-GEFs in endothelial cells and in multiple cancer cells (Grossmann et al., 2013; Hu et al., 2012; Morishige et al., 2008; Zhu et al., 2012), and both ARF-GEFs are expressed in human uveal melanoma tissues (Figure S4A). Knockdown of *GEP100* (Figure 4A), but not *ARNO* (Figure S4B), reduced ARF6-GTP levels by 60% in uveal melanoma cells. Knockdown of *GEP100* resulted in 50% inhibition of cell proliferation and 80% inhibition in anchorage-independent colony growth (Figure 4B and 4C), mimicking the cellular phenotypes of *ARF6* knockdown. Similar to the silencing of *ARF6* and *GNAQ*, knockdown of *GEP100* also inhibited PLC-PKC, Rac1/RhoA, YAP, and β-catenin signaling, as evidenced by decreased activation of the downstream effectors and reduced nuclear localization and transcriptional activity of YAP and β-catenin (Figures S4C–S4L). We hypothesized that oncogenic GNAQ and GEP100 might form a complex that activates ARF6 in uveal melanoma cells, because such complexes have been shown to occur following ectopic expression of Gαq and GEP100 in HEK293T cells (Giguere et al., 2006; Laroche et al., 2007). Immunoprecipitation of GNAQ from uveal melanoma cells harboring

the activating mutation co-precipitated GEP100 (Figure 4D), suggesting the existence of a $GNAQ^{Q209L}$-GEP100 complex.

ARF6 exerts its effect on constitutive GNAQ signaling by controlling $GNAQ^{Q209L}$ intracellular localization

ARF6 has a known role in endocytosis of GPCRs (Chen et al., 2003; Hunzicker-Dunn et al., 2002), and GPCRs and Gα proteins are known to traffic between the plasma membrane and early endosomes (Calebiro et al., 2009; Ferrandon et al., 2009; Hynes et al., 2004; Irannejad et al., 2013; Scarselli and Donaldson, 2009; Van Dyke, 2004; Zheng et al., 2004). To examine whether ARF6 might control activated GNAQ signaling through a similar protein trafficking mechanism, we knocked down *ARF6* in Mel92.1 and Mel202 cells and assessed intracellular localization of GNAQ using both immunocytofluorescence and cell fractionation analysis. Upon *ARF6* silencing, there was an increase in GNAQ localized to the plasma membrane with a concomitant reduction of GNAQ in the cytosol and cytoplasmic vesicles (Figure 5). *GEP100* knockdown likewise exhibited a shift of GNAQ localization from the cytosol and cytoplasmic vesicles to the plasma membrane (Figure S5A and S5B). Silencing of other human ARF family members did not cause appreciable intracellular relocalization of GNAQ (Figure S5C), thus suggesting that this function is specific to ARF6. Cumulatively, these results suggest that activated ARF6 directs GNAQ to the cytoplasmic vesicles, leading to an increase in signaling of downstream oncogenic pathways.

NAV-2729, a direct inhibitor of ARF6, mimics ARF6 knockdown in cell function assays

Our finding that ARF6 acts as an immediate downstream effector of the uveal melanoma GNAQ/GEP100 complex that controls all of the currently recognized signaling pathways governed by oncogenic Gαq compelled us to investigate whether chemical inhibitors of ARF6 activation might provide an effective pharmacologic treatment of uveal melanoma. To our knowledge, no direct inhibitors of ARF6 have been published or are commercially available. Therefore, ARF-GEF inhibitors, such as SecinH3, have been used as surrogates for ARF6 inhibition in past studies (Hafner et al., 2006; Grossmann et al., 2013). However, ARNO, a target for SecinH3 inhibition, promotes epidermal growth factor receptor activation independent of its ARF-GEF activity (Bill et al., 2010), so inhibiting ARF-GEFs rather than ARF6 directly could lead to off-target effects. Therefore, it is imperative to find direct ARF6 inhibitors that can reduce these unintended consequences. To identify such inhibitors, a high throughput screen (HTS) based on a fluorometric biochemical assay was devised to identify chemically tractable, reversible, allosteric inhibitors that target ARF6 directly (Figures 6A and S6A–S6C). The requirement for an allosteric, non-nucleotide-competitive mode of action was dictated by intracellular concentrations of GTP, which are approximately 100 μM. A comparative evaluation of more than 20 chemical series and singleton HTS hits from the DIVERSet-EXP collection (Chuprina et al., 2010) of approximately 50,000 compounds (ChemBridge) identified the pyrazolopyrimidinone compound NAV-2729 (Figures 6B and S6) as the most promising ARF6 chemical probe candidate. This compound was selected for further evaluation based on the following properties: i) low micromolar potency with IC50 values of 1.0 μM and 3.4 μM determined using fluorometric and orthogonal radiometric ARF6 nucleotide exchange assays,

respectively (Figure 6C); ii) direct inhibition of ARF6 as evidenced by nearly equipotent inhibitory effects towards spontaneous and ARF-GEF-catalyzed ARF6 nucleotide exchange (Figure 6D); iii) a non-nucleotide competitive mechanism supported by the lack of dependence of inhibitory potency on the nucleotide concentration (Figure 6E); iv) high selectivity as evidenced by the lack of inhibitory effects for all other human ARF family members, as well as other small GTPases, such as RhoA, Rac1, H-Ras, and Cdc42 at NAV-2729 concentrations up to 50 μM (Figure S6D–S6K); v) reversible inhibition (Figure 6F); and vi) overall chemical tractability including apparent lack of commonly recognized reactive and "frequent hitter" functionalities (Baell and Holloway, 2010).

The proposed direct inhibitory mechanism of NAV-2729 agrees well with the results of molecular docking studies using a structural homology model of the ARF6/ARF-GEF complex (Figure 6G). The model predicts association of NAV-2729 with ARF6 in its GEF-binding area, which does not overlap with the nucleotide-binding pocket. A hydrogen bond between the inhibitor carbonyl group and ε-amino group of ARF6 Lys58 residue, as well as the interaction of its nitrophenyl moiety with a hydrophobic pocket formed by aromatic side chains of ARF6 residues Phe47, Trp62, Trp74, and Tyr77 make major contributions to the inhibitor binding energy (Figure S6L). Most importantly, NAV-2729 exhibited a spectrum of biological activities in uveal melanoma cells that are predicted for an ARF6 inhibitor. Treatment of Mel92.1 and Mel202 cells with NAV-2729 inhibited ARF6 activation (Figure 6H) and mimicked *ARF6* and *GEP100* knockdown by driving GNAQ from the cytoplasmic vesicles to the plasma membrane (Figure 6I and 6J) and reducing anchorage-independent colony growth (Figure 6K). NAV-2729 also blocked all of the known downstream signaling pathways of oncogenic GNAQ, including PLC/PKC, Rho/Rac, YAP, and β-catenin (Figure 7).

ARF6 is a potential therapeutic target for oncogenic GNAQ-driven tumors

The finding that the activation state of ARF6 regulates multiple oncogenic GNAQ signaling pathways by controlling the intracellular localization of $GNAQ^{Q209L}$ suggested that ARF6 may be a viable therapeutic target for GNAQ-mediated tumorigenesis. We tested this hypothesis in an orthotopic xenograft mouse model of uveal melanoma. Stable uveal melanoma cells expressing either short hairpin RNAs (shRNA) directed against ARF6 or a non-specific control sequence were generated by lentiviral infection of Mel202 cells. These cells were injected into the posterior vitreous chamber of the eyes of immunocompromised nude mice. Tumor incidence and size were markedly decreased in mice injected with Mel202 cells expressing ARF6 shRNA compared to mice injected with cells expressing control shRNA (Figure 8A and 8B). Systemic treatment by intraperitoneal injection of the direct ARF6 inhibitor NAV-2729 also significantly reduced uveal melanoma tumor establishment and growth in an orthotopic xenograft mouse model (Figure 8C and 8D). No signs of toxicity were observed in these studies or in other studies in which the drug was used at the same dosage (Figure S7, Tables S1–S3). Collectively, these results suggest that the pharmacological inhibition of ARF6 may represent an effective therapeutic approach to the treatment of uveal melanoma and possibly other cancers driven by activating Gα mutations.

DISCUSSION

Activated oncogenes such as Gα proteins or members of the RAS superfamily of GTPases act through central signaling nodes that subsequently trigger multiple molecular events that together induce cancer initiation and invasion (O'Hayre et al., 2014; Pylayeva-Gupta et al., 2011). Previous studies have shown that activating mutations in either GNAQ or GNA11 promote PLC/PCK and Rac/Rho signaling, leading to both the activation of ERK, p38, JNK, and YAP and subsequent AP-1- and YAP/TEAD-mediated transcription (Feng et al., 2014; Vaque et al., 2013; Wu et al., 2012b; Yu et al., 2014). In the present study, we have expanded the number of signaling pathways that are known to be regulated by an activated Gαq protein to include an ARF6-β-catenin pathway in which activated ARF6 promotes the release and subsequent translocation of membrane-bound β-catenin to the nucleus where it induces transcription. By employing biochemical and cellular assays and a newly identified small molecule inhibitor, we also show that a $GNAQ^{Q209L}$-GEP100 complex activates ARF6, which functions as an immediate downstream effector to induce the PLC/PKC and Rho/Rac signaling pathways that lead to AP-1 and YAP/TEAD-mediated transcription (Figure 8E). Thus, the activation of ARF6 controls all of the currently known oncogenic pathways mediated by Gαq activating mutations.

Our data suggest that activated ARF6 controls GNAQ and β-catenin signaling by regulating protein trafficking between intracellular compartments. Oncogenic GNAQ forms a protein complex with GEP100, which activates ARF6 to promote the redistribution of cell surface GNAQ to cytoplasmic vesicles. GNAQ signaling appears to primarily occur in these vesicles, because knockdown of ARF6 or GEP100 or chemical inhibition of ARF6 induces the relocalization of GNAQ from the cytoplasm to the plasma membrane with a concomitant decrease in signaling of all GNAQ-mediated pathways. Palmitoylation of GNAQ may contribute to its association with cellular membranes (Wedegaertner et al., 1993). Although signaling from G proteins such as Gα and RAS proteins have traditionally been thought to occur only at the plasma membrane, more recent studies have challenged this view, suggesting that signaling can also derive from cytoplasmic vesicles (Calebiro et al., 2009; Fehrenbacher et al., 2009; Ferrandon et al., 2009; Hancock, 2003; Hynes et al., 2004; Irannejad et al., 2013; Irannejad and von Zastrow, 2014; Scarselli and Donaldson, 2009; Van Dyke, 2004; Vilardaga et al., 2014; Zheng et al., 2004). Our data agree with these recent studies but unexpectedly suggest that most of the signaling from active GNAQ in uveal melanoma emanates from cytoplasmic vesicles rather than the plasma membrane. These results, coupled with previous work suggesting that maximal oncogenic H-RAS signaling requires endocytosis and endocytic recycling (Roy et al., 2002), suggest that the intracellular location of an oncogene may determine its level of activity and that blocking the trafficking of an oncogene to its primary signaling center may effectively diminish its activity. In the case of GNAQ and H-RAS, the primary signaling center appears to be in cytoplasmic vesicles. The activation of ARF6 by oncogenic GNAQ also leads to the release of β-catenin from the plasma membrane and its subsequent transportation to the nucleus where it induces gene transcription and helps to promote uveal melanoma cell proliferation. This result is consistent with our previous study in cutaneous melanoma, which demonstrated a similar

relocalization of β-catenin and increased β-catenin-mediated transcription following stimulation of the FZD4/LRP6 co-receptor complex with WNT5A (Grossmann et al., 2013).

Our discovery that ARF6 is an immediate downstream effector of the $GNAQ^{Q209L}$-GEP100 complex suggests that targeting ARF6 with a single small molecule may inhibit all of the currently known Gαq-mediated oncogenic signaling pathways. The necessity and sufficiency of ARF6 activation in orchestrating activated Gαq oncogenic signaling also reveals a strategy to blunt cancer initiation and progression, not just tumor invasion and metastasis. We provide evidence that ARF6 is an actionable node suitable for further development as a therapeutic target by identifying a direct inhibitor of ARF6 that reduces tumor establishment and growth in a xenograft model of uveal melanoma.

Uveal melanoma is a devastating cancer and serves as the prototype for activated Gα protein-mediated cancers. Current treatment relies on surgery and radiation for localized disease, but there is no effective systemic therapy for advanced disease (Harbour, 2012). The identification of ARF6 as a signaling partner of GNAQ, offers a target for treatment regimens that has implications extending beyond Gαq proteins and uveal melanoma to other cancers harboring activated Gα oncogenes, such as pancreatic and biliary cancers (O'Hayre et al., 2013). Directly targeting certain oncogenes, e.g., activated RAS GTPase, has been challenging (Spiegel et al., 2014; Stephen et al., 2014), although recent advances have been made (Lim et al., 2014; Ostrem et al., 2013). Approaches that individually inhibit each arm of an activated oncogenic pathway have been adopted but are inefficient, spurring interest in combination trials as an alternate approach (Thompson, 2013). By illuminating how a specific activated Gα oncogene orchestrates multiple divergent downstream signaling arms through a single effector, our work suggests that targeting such primary nodal points in the signaling pathways of other GTPases could provide an effective method for combatting oncogenesis and tumor establishment.

EXPERIMENTAL PROCEDURES

Detailed protocols for each of the sections below can be found in the Supplemental Experimental Procedures section of Supplemental Information.

Cell lines, proliferation assay, and anchorage-independent colony growth assay

Mel92.1 and Mel202 uveal melanoma cells were maintained in RPMI 1640 supplemented with 10% fetal bovine serum (FBS). HEK293T cells were purchased from ATCC and maintained in DMEM supplemented with 10% FBS. Cell proliferation assays were performed using CyQUANT (Invitrogen) according to the manufacturer's instructions. Anchorage-independent colony growth was quantified by the CytoSelect 96-Well Cell Transformation Assay (Cell Biolabs) as per manufacturer's instructions.

RNA interference, plasmids, transfections, lentiviral transduction, and qRT-PCR

siRNA duplexes (20 nmol) were transfected into uveal melanoma cells using Lipofectamine RNAiMAX (Invitrogen). The coding regions for GNAQ and $GNAQ^{Q209L}$ (Missouri S&T cDNA Resource Center) were cloned into pcDNA3.1 for N-terminal MYC-tagging. HEK293T cells were transfected using Lipofectamine LTX (Invitrogen). Mel202 cells were

transduced with lentiviruses expressing *ARF6* shRNA (Sigma) and selected for stable expression. Rescue experiments were performed as described in Supplemental Experimental Procedures. qRT-PCR was performed with the Applied Biosystems 7900HT and QuantiTect SYBR Green PCR kit (Qiagen).

ARF6/RhoA/Rac1 pull-downs, immunoblots, immunoprecipitation, cell fractionation, PLC assay, luciferase assay, and immunofluorescence staining

ARF6-GTP pull-downs were performed with Arf6 Activation Assay Kit (Cell Biolabs) and Rac1/RhoA-GTP pull-downs were prepared with Rac1 Activation Assay Kit/RhoA Activation Assay Kit (Millipore) according to the manufacturer's instructions. Immunoprecipitation was performed as previously described (Grossmann et al., 2013). For immunoblotting, primary antibodies were diluted in 5% NFDM or 5% BSA in PBS or TBS plus 0.1% Tween 20 and incubated overnight at 4°C. Plasma membrane or total membrane fraction was isolated with Plasma Membrane Protein Extraction Kit (Abcam) and cytosolic/nuclear fractions were prepared with NE-PER Nuclear and Cytoplasmic Extraction Reagents (Thermo Scientific) according to the manufacturer's instructions. All antibodies for immunoblots, immunoprecipitation, and immunocytofluorescence staining are listed in table format in Supplemental Experimental Procedures. Scanning densitometry was used for immunoblot quantification. β-catenin- and AP-1-mediated transcriptional activities in uveal melanoma cells were assayed using lentivirally transduced cells that stably express the TOPflash-based 7TFP luciferase reporter (Addgene) (Fuerer and Nusse, 2010) or AP-1 luciferase reporter (QIAGEN). PLC activity was determined using phosphoinositide turnover assay as described by others (Vaque et al., 2013).

For immunofluorescence staining studies, Mel202 and Mel92.1 cells were transfected with ARF6, GNAQ, and control siRNAs and later fixed with formalin and then thoroughly washed with TBS. The fixed cells were treated with primary antibodies overnight at 4°C in TBS containing 1% BSA and 0.1% Saponin. Cells were washed and secondary Alexafluor-conjugated secondary antibody was applied for 1 h at room temperature. The cells were washed, DAPI anti-Fade medium was added, and randomly selected fields were imaged at 1200x on an Olympus FV1000 confocal microscope.

Human uveal melanoma patient samples

These studies were done in accordance with a protocol approved by the University of Miami Institutional Review Board and informed consent was obtained from all patients. Primary human uveal melanoma samples were collected at the time of enucleation as previously described (Onken et al., 2007).

Orthotopic xenograft mouse model of uveal melanoma

All animal studies were performed in accordance with a protocol approved by the University of Utah Institutional Animal Care and Use Committee. Nude mice were anesthetized and 10^5 Mel202 cells were injected into the posterior chamber of eye. For systemic small molecule treatment, intraperitoneal injections of either 30mg/kg NAV-2729 or control DMSO were provided each day. At 5 weeks, the mice were sacrificed and the eyes were

collected and treated for histology by a board certified pathologist who was blinded to treatment groups.

Recombinant Protein Expression and Purification

His-tagged proteins were purified from bacterial cultures to apparent homogeneity as described (Grossmann et al., 2013). ARF6 was converted to the GDP-bound form.

Toxicity Studies

See Supplemental Experimental Procedures.

Fluorometric Nucleotide Exchange Assay

GDP to GTP exchange on ARF6 and other small GTPases was monitored in a 96-well format high-throughput screen (HTS) using GTP-BODIPY FL (Life Technologies) by measuring increases in fluorescence intensity on a plate reader (excitation 490 nm and emission 520 nm). A DIVERSet-EXP library of compounds (ChemBridge) was used at 10 μM. The selectivity panel included 8 other N-terminally-tagged small GTPases that were produced in-house or purchased from Cytoskeleton.

Radiometric Nucleotide Exchange Assay

HTS hits were confirmed using radiometric assay for ARF6 nucleotide exchange in an assay mix similar to the used in the fluorometric nucleotide exchange assay, except that 50 nM [^{35}S]-GTPγS (2μCi/ml) replaced GTP-BODIPY FL.

Synthetic Methods

See Supplemental Experimental Procedures.

Molecular Modeling

Molecular modeling was performed using program package ICM-Pro (MolSoft, LLS, San Diego, CA) with the crystal structure of ARF1 (18–181)-GDP—ARNO—brefeldin A (Protein Data Bank ID 1S9D) (Renault et al., 2003) being used as a template to build the ARF6 (14–175) structures.

Statistical Analyses

Statistical analyses were performed using GraphPad Prism 6.0f. t-tests, multiple comparisons tests, nonparametric tests, and 95% confidence intervals were employed as appropriate.

Supplementary Material

Refer to Web version on PubMed Central for supplementary material.

Acknowledgments

We thank S. Holmen, T. Oliver, C. Murtaugh, J. Christian, A. Bild, W. Sundquist, C. Hill, J. Kaplan, D. Ward, M. Babst, E. Jorgensen, M. Sanguinetti, and M. E. Hartnett for critical reading of the manuscript, D. Ward for technical advice, and D.Y.L. lab members for critical discussion of the manuscript. We thank C. Rodesch and the Cell

Imaging Core Facility at the University of Utah for technical assistance, B. Anderson and the Huntsman Cancer Institute Biorepository and Molecular Pathology Shared Resources facility for preparation of tissues for histology, and D. Lim for assistance with figures. This work was funded by grants to D.Y.L., K.O., and J.W.H. from the National Institutes of Health (R01CA163970, R01NS080893, U54HL112311, R01HL077671, R0LHL084516, R01AR064788, UL1TR000105, U01NS083573, R43EY022516, R43AR063509, and R01CA125970), American Asthma Foundation (09-0172), the Burroughs Wellcome Fund (Clinical Scientist Award in Translational Medicine), and the Ben B. and Iris M. Margolis Foundation. D.Y.L. is co-founder and Chief Scientific Officer of Navigen, Inc. K.O., Z.T., C.D, A.B., M.S., and A.L.M. are employees of Navigen, Inc.

REFERENCES

Baell JB, Holloway GA. New substructure filters for removal of pan assay interference compounds (PAINS) from screening libraries and for their exclusion in bioassays. J Med Chem. 2010; 53:2719–2740. [PubMed: 20131845]

Berstein G, Blank JL, Smrcka AV, Higashijima T, Sternweis PC, Exton JH, Ross EM. Reconstitution of agonist-stimulated phosphatidylinositol 4,5-bisphosphate hydrolysis using purified m1 muscarinic receptor, Gq/11, and phospholipase C-beta 1. J Biol Chem. 1992; 267:8081–8088. [PubMed: 1341877]

Bill A, Schmitz A, Albertoni B, Song JN, Heukamp LC, Walrafen D, Thorwirth F, Verveer PJ, Zimmer S, Meffert L, et al. Cytohesins are cytoplasmic ErbB receptor activators. Cell. 2010; 143:201–211. [PubMed: 20946980]

Blank JL, Ross AH, Exton JH. Purification and characterization of two G-proteins that activate the beta 1 isozyme of phosphoinositide-specific phospholipase C. Identification as members of the Gq class. J Biol Chem. 1991; 266:18206–18216. [PubMed: 1655741]

Bose A, Cherniack AD, Langille SE, Nicoloro SM, Buxton JM, Park JG, Chawla A, Czech MP. G(alpha)11 signaling through ARF6 regulates F-actin mobilization and GLUT4 glucose transporter translocation to the plasma membrane. Mol Cell Biol. 2001; 21:5262–5275. [PubMed: 11438680]

Calebiro D, Nikolaev VO, Gagliani MC, de Filippis T, Dees C, Tacchetti C, Persani L, Lohse MJ. Persistent cAMP-signals triggered by internalized G-protein-coupled receptors. PLoS biology. 2009; 7:e1000172. [PubMed: 19688034]

Chen B, Dodge ME, Tang W, Lu J, Ma Z, Fan CW, Wei S, Hao W, Kilgore J, Williams NS, et al. Small molecule-mediated disruption of Wnt-dependent signaling in tissue regeneration and cancer. Nature chemical biology. 2009; 5:100–107. [PubMed: 19125156]

Chen W, ten Berge D, Brown J, Ahn S, Hu LA, Miller WE, Caron MG, Barak LS, Nusse R, Lefkowitz RJ. Dishevelled 2 recruits beta-arrestin 2 to mediate Wnt5A–stimulated endocytosis of Frizzled 4. Science. 2003; 301:1391–1394. [PubMed: 12958364]

Chuprina A, Lukin O, Demoiseaux R, Buzko A, Shivanyuk A. Drug- and lead-likeness, target class, and molecular diversity analysis of 7.9 million commercially available organic compounds provided by 29 suppliers. J Chem Inf Model. 2010; 50:470–479. [PubMed: 20297844]

Clevers H. Wnt/beta-catenin signaling in development and disease. Cell. 2006; 127:469–480. [PubMed: 17081971]

D'Souza-Schorey C, Li G, Colombo MI, Stahl PD. A regulatory role for ARF6 in receptor-mediated endocytosis. Science. 1995; 267:1175–1178. [PubMed: 7855600]

Dorsam RT, Gutkind JS. G-protein-coupled receptors and cancer. Nat Rev Cancer. 2007; 7:79–94. [PubMed: 17251915]

Fehrenbacher N, Bar-Sagi D, Philips M. Ras/MAPK signaling from endomembranes. Molecular oncology. 2009; 3:297–307. [PubMed: 19615955]

Feng X, Degese MS, Iglesias-Bartolome R, Vaque JP, Molinolo AA, Rodrigues M, Zaidi MR, Ksander BR, Merlino G, Sodhi A, et al. Hippo-Independent Activation of YAP by the GNAQ Uveal Melanoma Oncogene through a Trio-Regulated Rho GTPase Signaling Circuitry. Cancer cell. 2014; 25:831–845. [PubMed: 24882515]

Ferrandon S, Feinstein TN, Castro M, Wang B, Bouley R, Potts JT, Gardella TJ, Vilardaga JP. Sustained cyclic AMP production by parathyroid hormone receptor endocytosis. Nature chemical biology. 2009; 5:734–742. [PubMed: 19701185]

Fuerer C, Nusse R. Lentiviral vectors to probe and manipulate the Wnt signaling pathway. PLoS One. 2010; 5:e9370. [PubMed: 20186325]

Giguere P, Rochdi MD, Laroche G, Dupre E, Whorton MR, Sunahara RK, Claing A, Dupuis G, Parent JL. ARF6 activation by Galpha q signaling: Galpha q forms molecular complexes with ARNO and ARF6. Cell Signal. 2006; 18:1988–1994. [PubMed: 16650966]

Griewank KG, Yu X, Khalili J, Sozen MM, Stempke-Hale K, Bernatchez C, Wardell S, Bastian BC, Woodman SE. Genetic and molecular characterization of uveal melanoma cell lines. Pigment Cell Melanoma Res. 2012; 25:182–187. [PubMed: 22236444]

Grossmann AH, Yoo JH, Clancy J, Sorensen LK, Sedgwick A, Tong Z, Ostanin K, Rogers A, Grossmann KF, Tripp SR, et al. The small GTPase ARF6 stimulates beta-catenin transcriptional activity during WNT5A-mediated melanoma invasion and metastasis. Science signaling. 2013; 6:ra14. [PubMed: 23462101]

Hancock JF. Ras proteins: different signals from different locations. Nat Rev Mol Cell Biol. 2003; 4:373–384. [PubMed: 12728271]

Harbour JW. The genetics of uveal melanoma: an emerging framework for targeted therapy. Pigment Cell Melanoma Res. 2012; 25:171–181. [PubMed: 22268848]

Hu B, Shi B, Jarzynka MJ, Yiin JJ, D'Souza-Schorey C, Cheng SY. ADP-ribosylation factor 6 regulates glioma cell invasion through the IQ-domain GTPase-activating protein 1-Rac1-mediated pathway. Cancer Res. 2009; 69:794–801. [PubMed: 19155310]

Hu Z, Du J, Yang L, Zhu Y, Yang Y, Zheng D, Someya A, Gu L, Lu X. GEP100/Arf6 is required for epidermal growth factor-induced ERK/Rac1 signaling and cell migration in human hepatoma HepG2 cells. PLoS One. 2012; 7:e38777. [PubMed: 22701712]

Huang SM, Mishina YM, Liu S, Cheung A, Stegmeier F, Michaud GA, Charlat O, Wiellette E, Zhang Y, Wiessner S, et al. Tankyrase inhibition stabilizes axin and antagonizes Wnt signalling. Nature. 2009; 461:614–620. [PubMed: 19759537]

Hunzicker-Dunn M, Gurevich VV, Casanova JE, Mukherjee S. ARF6: a newly appreciated player in G protein-coupled receptor desensitization. FEBS Lett. 2002; 521:3–8. [PubMed: 12067715]

Hynes TR, Mervine SM, Yost EA, Sabo JL, Berlot CH. Live cell imaging of Gs and the beta2-adrenergic receptor demonstrates that both alphas and beta1gamma7 internalize upon stimulation and exhibit similar trafficking patterns that differ from that of the beta2-adrenergic receptor. J Biol Chem. 2004; 279:44101–44112. [PubMed: 15297467]

Irannejad R, Tomshine JC, Tomshine JR, Chevalier M, Mahoney JP, Steyaert J, Rasmussen SG, Sunahara RK, El-Samad H, Huang B, von Zastrow M. Conformational biosensors reveal GPCR signalling from endosomes. Nature. 2013; 495:534–538. [PubMed: 23515162]

Irannejad R, von Zastrow M. GPCR signaling along the endocytic pathway. Curr Opin Cell Biol. 2014; 27:109–116. [PubMed: 24680436]

Ji H, Wang J, Nika H, Hawke D, Keezer S, Ge Q, Fang B, Fang X, Fang D, Litchfield DW, et al. EGF-induced ERK activation promotes CK2-mediated disassociation of alpha-Catenin from beta-Catenin and transactivation of beta-Catenin. Mol Cell. 2009; 36:547–559. [PubMed: 19941816]

Kahn RA, Gilman AG. Purification of a protein cofactor required for ADP-ribosylation of the stimulatory regulatory component of adenylate cyclase by cholera toxin. J Biol Chem. 1984; 259:6228–6234. [PubMed: 6327671]

Khalili JS, Yu X, Wang J, Hayes BC, Davies MA, Lizee G, Esmaeli B, Woodman SE. Combination small molecule MEK and PI3K inhibition enhances uveal melanoma cell death in a mutant GNAQ- and GNA11-dependent manner. Clinical cancer research : an official journal of the American Association for Cancer Research. 2012; 18:4345–4355. [PubMed: 22733540]

Laroche G, Giguere PM, Dupre E, Dupuis G, Parent JL. The N-terminal coiled-coil domain of the cytohesin/ARNO family of guanine nucleotide exchange factors interacts with Galphaq. Molecular and cellular biochemistry. 2007; 306:141–152. [PubMed: 17846866]

Li M, Wang J, Ng SS, Chan CY, He ML, Yu F, Lai L, Shi C, Chen Y, Yew DT, et al. Adenosine diphosphate-ribosylation factor 6 is required for epidermal growth factor-induced glioblastoma cell proliferation. Cancer. 2009; 115:4959–4972. [PubMed: 19642173]

Lim SM, Westover KD, Ficarro SB, Harrison RA, Choi HG, Pacold ME, Carrasco M, Hunter J, Kim ND, Xie T, et al. Therapeutic targeting of oncogenic K-Ras by a covalent catalytic site inhibitor. Angew Chem Int Ed Engl. 2014; 53:199–204. [PubMed: 24259466]

Marinissen MJ, Gutkind JS. G-protein-coupled receptors and signaling networks: emerging paradigms. Trends in pharmacological sciences. 2001; 22:368–376. [PubMed: 11431032]

Morishige M, Hashimoto S, Ogawa E, Toda Y, Kotani H, Hirose M, Wei S, Hashimoto A, Yamada A, Yano H, et al. GEP100 links epidermal growth factor receptor signalling to Arf6 activation to induce breast cancer invasion. Nat Cell Biol. 2008; 10:85–92. [PubMed: 18084281]

Muralidharan-Chari V, Hoover H, Clancy J, Schweitzer J, Suckow MA, Schroeder V, Castellino FJ, Schorey JS, D'Souza-Schorey C. ADP-ribosylation factor 6 regulates tumorigenic and invasive properties in vivo. Cancer Res. 2009; 69:2201–2209. [PubMed: 19276388]

Nakashima M, Miyajima M, Sugano H, Iimura Y, Kato M, Tsurusaki Y, Miyake N, Saitsu H, Arai H, Matsumoto N. The somatic GNAQ mutation c.548G>A (p.R183Q) is consistently found in Sturge-Weber syndrome. Journal of human genetics. 2014; 59:691–693. [PubMed: 25374402]

O'Hayre M, Degese MS, Gutkind JS. Novel insights into G protein and G protein-coupled receptor signaling in cancer. Curr Opin Cell Biol. 2014; 27C:126–135. [PubMed: 24508914]

O'Hayre M, Vazquez-Prado J, Kufareva I, Stawiski EW, Handel TM, Seshagiri S, Gutkind JS. The emerging mutational landscape of G proteins and G-protein-coupled receptors in cancer. Nat Rev Cancer. 2013; 13:412–424. [PubMed: 23640210]

Onken MD, Worley LA, Person E, Char DH, Bowcock AM, Harbour JW. Loss of heterozygosity of chromosome 3 detected with single nucleotide polymorphisms is superior to monosomy 3 for predicting metastasis in uveal melanoma. Clinical cancer research : an official journal of the American Association for Cancer Research. 2007; 13:2923–2927. [PubMed: 17504992]

Ostrem JM, Peters U, Sos ML, Wells JA, Shokat KM. K-Ras(G12C) inhibitors allosterically control GTP affinity and effector interactions. Nature. 2013; 503:548–551. [PubMed: 24256730]

Palacios F, Price L, Schweitzer J, Collard JG, D'Souza-Schorey C. An essential role for ARF6-regulated membrane traffic in adherens junction turnover and epithelial cell migration. EMBO J. 2001; 20:4973–4986. [PubMed: 11532961]

Pellon-Cardenas O, Clancy J, Uwimpuhwe H, D'Souza-Schorey C. ARF6-regulated endocytosis of growth factor receptors links cadherin-based adhesion to canonical Wnt signaling in epithelia. Mol Cell Biol. 2013; 33:2963–2975. [PubMed: 23716594]

Pylayeva-Gupta Y, Grabocka E, Bar-Sagi D. RAS oncogenes: weaving a tumorigenic web. Nat Rev Cancer. 2011; 11:761–774. [PubMed: 21993244]

Renault L, Guibert B, Cherfils J. Structural snapshots of the mechanism and inhibition of a guanine nucleotide exchange factor. Nature. 2003; 426:525–530. [PubMed: 14654833]

Reya T, Clevers H. Wnt signalling in stem cells and cancer. Nature. 2005; 434:843–850. [PubMed: 15829953]

Roy S, Wyse B, Hancock JF. H-Ras signaling and K-Ras signaling are differentially dependent on endocytosis. Mol Cell Biol. 2002; 22:5128–5140. [PubMed: 12077341]

Scarselli M, Donaldson JG. Constitutive internalization of G protein-coupled receptors and G proteins via clathrin-independent endocytosis. J Biol Chem. 2009; 284:3577–3585. [PubMed: 19033440]

Shirley MD, Tang H, Gallione CJ, Baugher JD, Frelin LP, Cohen B, North PE, Marchuk DA, Comi AM, Pevsner J. Sturge-Weber syndrome and port-wine stains caused by somatic mutation in GNAQ. N Engl J Med. 2013; 368:1971–1979. [PubMed: 23656586]

Shoushtari AN, Carvajal RD. GNAQ and GNA11 mutations in uveal melanoma. Melanoma Res. 2014; 24:525–534. [PubMed: 25304237]

Spiegel J, Cromm PM, Zimmermann G, Grossmann TN, Waldmann H. Small-molecule modulation of Ras signaling. Nature chemical biology. 2014; 10:613–622. [PubMed: 24929527]

Stephen AG, Esposito D, Bagni RK, McCormick F. Dragging ras back in the ring. Cancer cell. 2014; 25:272–281. [PubMed: 24651010]

Thompson H. US National Cancer Institute's new Ras project targets an old foe. Nat Med. 2013; 19:949–950. [PubMed: 23921727]

Van Dyke RW. Heterotrimeric G protein subunits are located on rat liver endosomes. BMC physiology. 2004; 4:1. [PubMed: 14711382]

Van Raamsdonk CD, Bezrookove V, Green G, Bauer J, Gaugler L, O'Brien JM, Simpson EM, Barsh GS, Bastian BC. Frequent somatic mutations of GNAQ in uveal melanoma and blue naevi. Nature. 2009; 457:599–602. [PubMed: 19078957]

Van Raamsdonk CD, Griewank KG, Crosby MB, Garrido MC, Vemula S, Wiesner T, Obenauf AC, Wackernagel W, Green G, Bouvier N, et al. Mutations in GNA11 in uveal melanoma. N Engl J Med. 2010; 363:2191–2199. [PubMed: 21083380]

Vaque JP, Dorsam RT, Feng X, Iglesias-Bartolome R, Forsthoefel DJ, Chen Q, Debant A, Seeger MA, Ksander BR, Teramoto H, Gutkind JS. A genome-wide RNAi screen reveals a Trio-regulated Rho GTPase circuitry transducing mitogenic signals initiated by G protein-coupled receptors. Mol Cell. 2013; 49:94–108. [PubMed: 23177739]

Vilardaga JP, Jean-Alphonse FG, Gardella TJ. Endosomal generation of cAMP in GPCR signaling. Nature chemical biology. 2014; 10:700–706. [PubMed: 25271346]

Wedegaertner PB, Chu DH, Wilson PT, Levis MJ, Bourne HR. Palmitoylation is required for signaling functions and membrane attachment of Gq alpha and Gs alpha. J Biol Chem. 1993; 268:25001–25008. [PubMed: 8227063]

Weinstein LS, Shenker A, Gejman PV, Merino MJ, Friedman E, Spiegel AM. Activating mutations of the stimulatory G protein in the McCune-Albright syndrome. N Engl J Med. 1991; 325:1688–1695. [PubMed: 1944469]

Wu X, Li J, Zhu M, Fletcher JA, Hodi FS. Protein kinase C inhibitor AEB071 targets ocular melanoma harboring GNAQ mutations via effects on the PKC/Erk1/2 and PKC/NF-kappaB pathways. Mol Cancer Ther. 2012a; 11:1905–1914. [PubMed: 22653968]

Wu X, Zhu M, Fletcher JA, Giobbie-Hurder A, Hodi FS. The protein kinase C inhibitor enzastaurin exhibits antitumor activity against uveal melanoma. PLoS One. 2012b; 7:e29622. [PubMed: 22253748]

Yu FX, Luo J, Mo JS, Liu G, Kim YC, Meng Z, Zhao L, Peyman G, Ouyang H, Jiang W, et al. Mutant Gq/11 Promote Uveal Melanoma Tumorigenesis by Activating YAP. Cancer cell. 2014; 25:822–830. [PubMed: 24882516]

Zheng B, Lavoie C, Tang TD, Ma P, Meerloo T, Beas A, Farquhar MG. Regulation of epidermal growth factor receptor degradation by heterotrimeric Galphas protein. Mol Biol Cell. 2004; 15:5538–5550. [PubMed: 15469987]

Zhu W, London NR, Gibson CC, Davis CT, Tong Z, Sorensen LK, Shi DS, Guo J, Smith MC, Grossmann AH, et al. Interleukin receptor activates a MYD88-ARNO-ARF6 cascade to disrupt vascular stability. Nature. 2012; 492:252–255. [PubMed: 23143332]

Highlights

- ARF6 is an immediate downstream effector of an activated GNAQ/GEP100 complex
- ARF6 acts as a node for all downstream signaling pathways induced by oncogenic GNAQ
- Maximal signaling occurs when GNAQ is shuttled to cytoplasmic vesicles
- Targeting nodes such as ARF6 provide an approach for treating recalcitrant cancers

SIGNIFICANCE

Activating mutations in G proteins, such as Gαq and RAS, drive oncogenesis in many cancers by triggering multiple downstream signaling pathways. However, these G proteins have proven elusive to therapeutic targeting and therefore most efforts have targeted each divergent pathway individually, thereby blocking only a subset of the critical pathways. We found that oncogenic GNAQ, a Gαq protein, induces its multiple signaling pathways through a single node—the small GTPase ARF6. Blocking ARF6 with a small molecule inhibitor reduces tumorigenesis in a mouse model of uveal melanoma. These results suggest that targeting proximal signaling nodes, rather than their upstream oncogenes or multiple downstream effectors, may be an effective strategy for treating cancers driven by recalcitrant oncogenes.

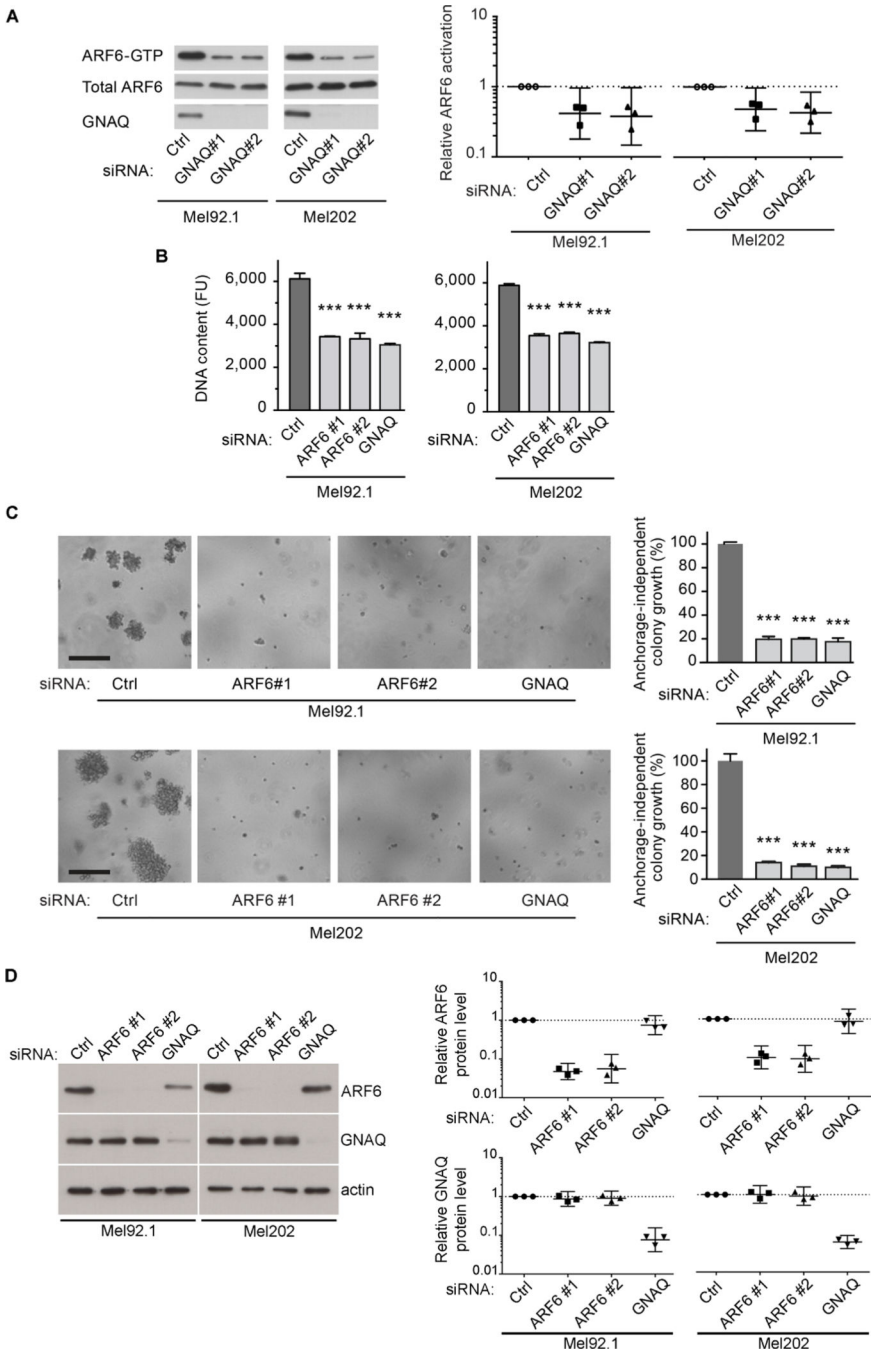

Figure 1. ARF6 is activated by oncogenic GNAQ and is required for uveal melanoma cell proliferation

(A) ARF6-GTP levels in uveal melanoma cells transfected with control (Ctrl), GNAQ#1, or GNAQ#2 siRNAs as assessed by immunoblotting and densitometry.

(B) Uveal melanoma cell proliferation following transfection with Ctrl, ARF6#1, ARF6#2, or GNAQ siRNAs as assessed by DNA content using CyQUANT and a fluorescence microplate reader. FU: Fluorescence Units.

(C) Anchorage-independent colony growth of cells transfected as in panel B. Percent DNA content relative to control. Scale bar: 250 μm.

(D) Specificity of ARF6 and GNAQ siRNAs shown by immunoblot.

Graphs in panels A and D show individual data points normalized to control along with geometric means and 95% confidence intervals (95% CI). 95% CIs that do not cross the dotted line at y=1 represent significant differences relative to the control at α=0.05. n=3. Data in panels B and C are represented as mean ± SD, n=3 experiments. One-way ANOVA, Dunnett's multiple comparisons test, ***$p < 0.001$.

See also Figure S1.

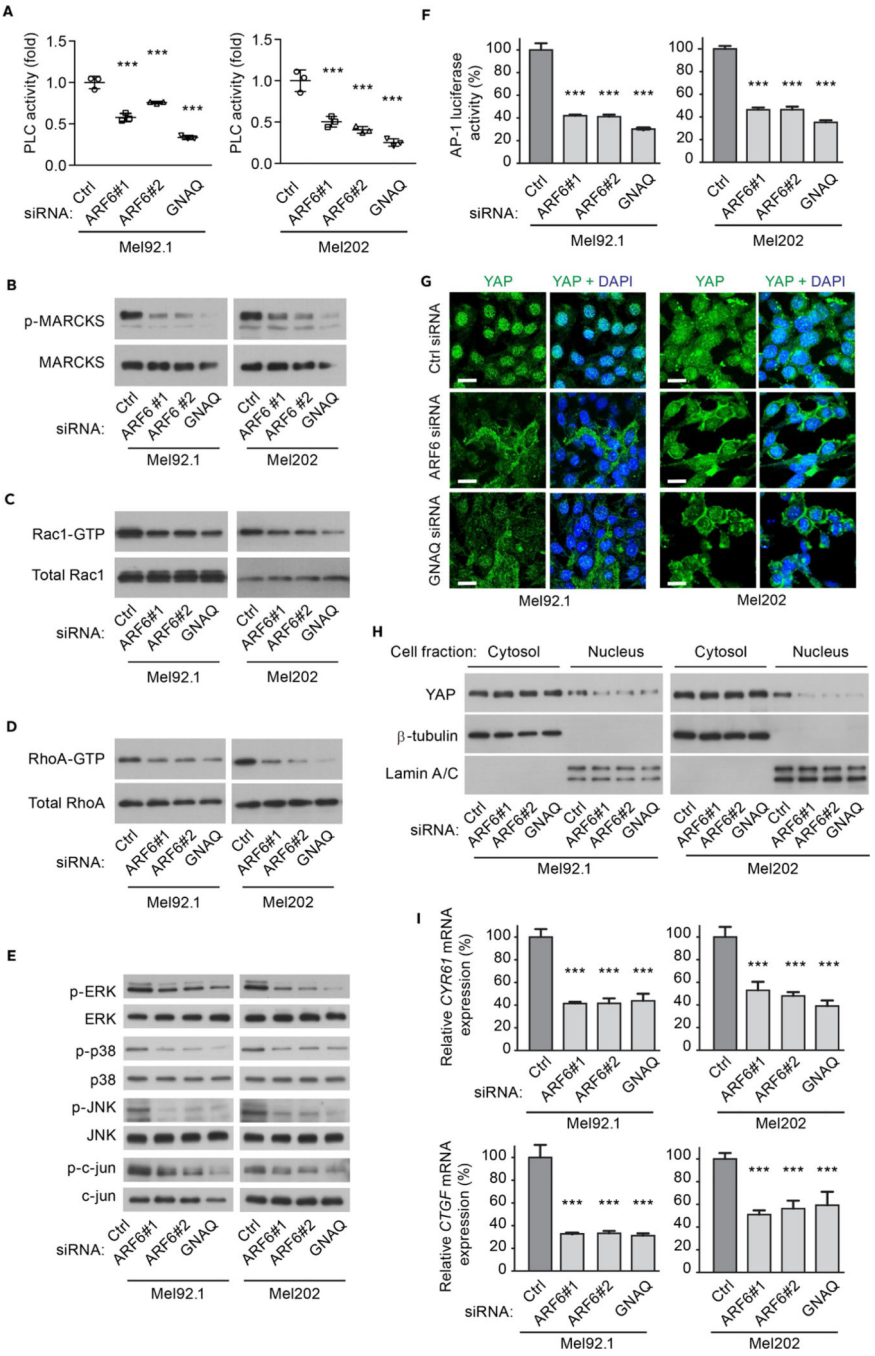

Figure 2. ARF6 is necessary for oncogenic GNAQ-induced PLC/PKC, Rac/Rho, MAPK, and YAP activation

(A) PLC phosphoinositide turnover assay in uveal melanoma cells transfected with control (Ctrl), ARF6#1, ARF6#2, or GNAQ siRNAs. n=3 experiments.

(B–E) Levels of p-MARCKS/MARCKS (B), Rac1-GTP/total Rac1 (C), RhoA-GTP/total RhoA (D), p-ERK/ERK, p-p38/p38, p-JNK/JNK, and p-c-jun/c-jun (E) as assessed by immunoblotting from cells transfected as in panel A.

(F) AP-1-mediated luciferase activities in uveal melanoma cells transfected with Ctrl, ARF6#1, ARF6#2, or GNAQ siRNAs.

(G–I) Examination of YAP activation in uveal melanoma cells following treatment with ARF6 or GNAQ siRNAs as illustrated by immunocytofluorescence (G), subcellular fractionation (H), and target gene expression (I). Scale bar: 30 μm. Data are represented as mean ± SD, n=3 experiments. One-way ANOVA, Dunnett's multiple comparisons test, ***$p < 0.001$.

See also Figure S2.

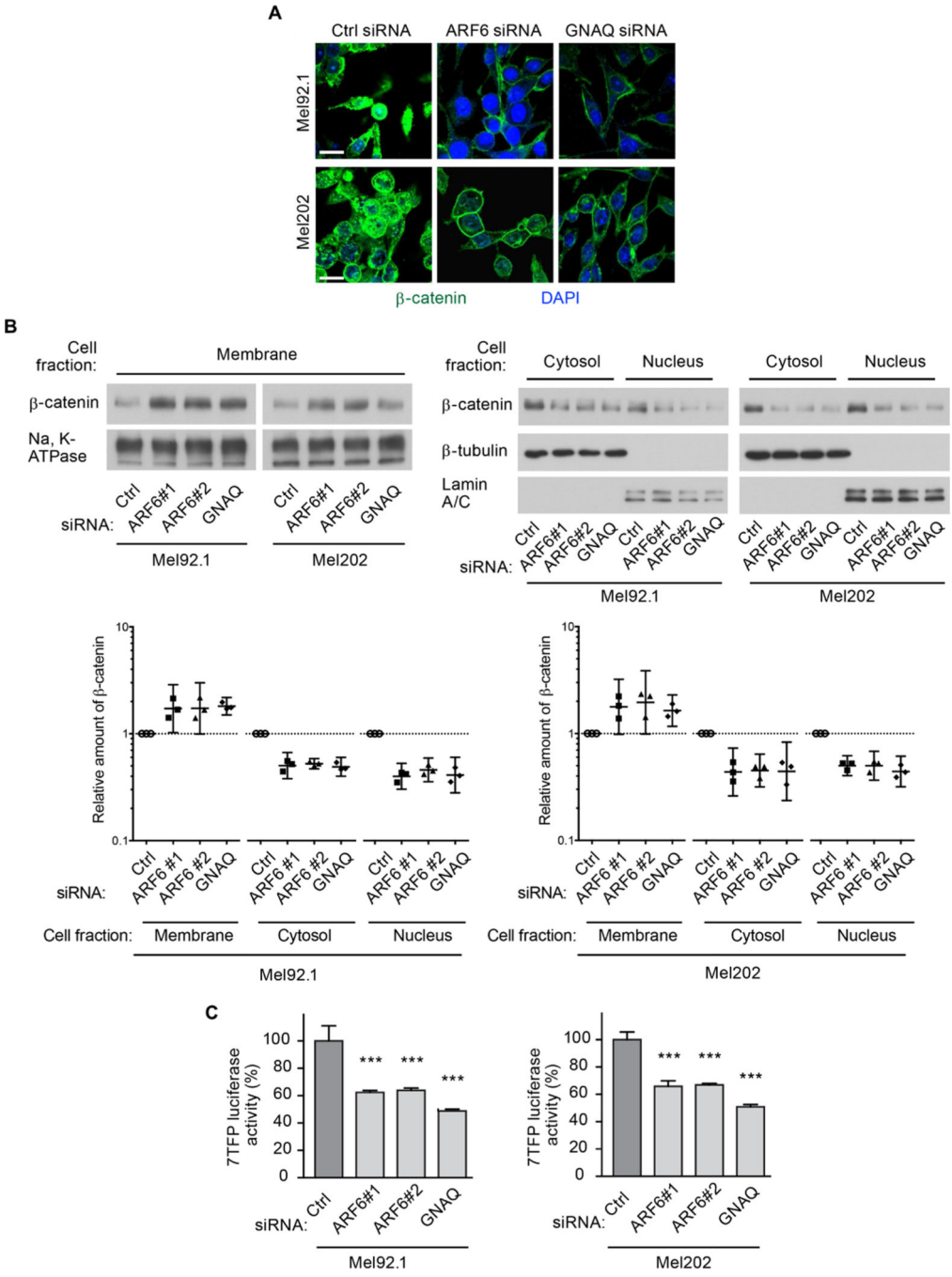

Figure 3. GNAQ and ARF6 control the subcellular localization and transactivation of β-catenin in uveal melanoma cells

(A) Immunocytofluorescent staining for β-catenin intracellular localization (green). Scale bar: 30 μm.

(B) Subcellular fractionation (membrane, cytosol, and nucleus) in Mel92.1 and Mel202 uveal melanoma cells transfected with control (Ctrl), ARF6#1, ARF6#2, or GNAQ siRNAs. Individual data points that have been normalized to the control are shown along with geometric means and 95% confidence intervals (CIs). 95% CIs that do not cross the dotted line at y=1 represent significant differences relative to the control at α=0.05.

(C) Luciferase reporter assays to measure β-catenin-mediated transcription following transfection of Mel92.1 or Mel202 cells with Ctrl, ARF6#1, ARF6#2, or GNAQ siRNAs. Data are represented as mean ± SD, n=3 experiments. One-way ANOVA, Dunnett's multiple comparisons test, ***$p < 0.001$.
See also Figures S3.

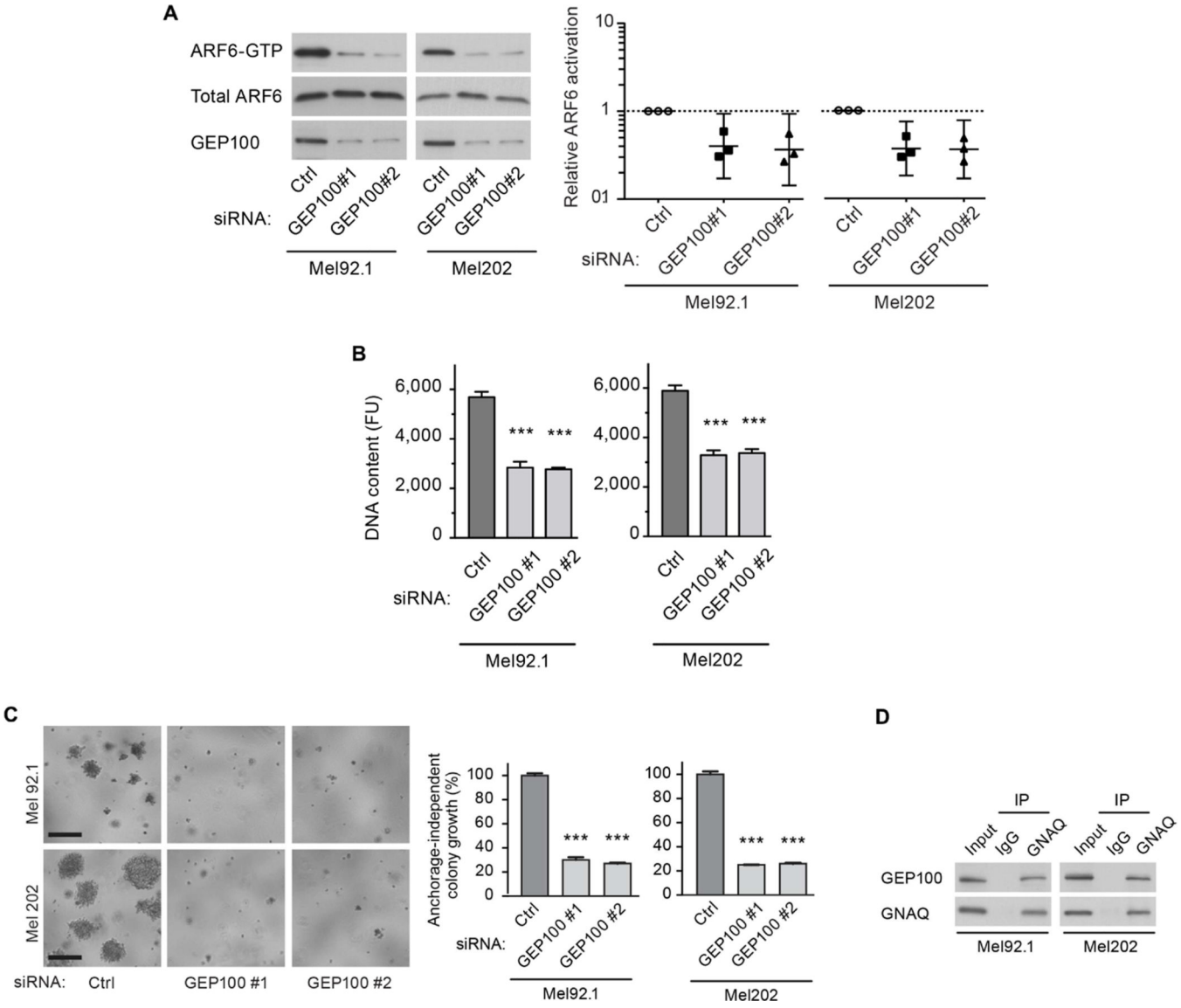

Figure 4. An oncogenic GNAQ-GEP100 complex activates ARF6 and is necessary for uveal melanoma cell proliferation

(A) ARF6-GTP levels in uveal melanoma cells transfected with control (Ctrl), GEP100#1, and GEP100#2 siRNAs as measured by pull-down assays and immunoblotting. Individual data points that have been normalized to the control are shown along with geometric means and 95% confidence intervals (CIs). 95% CIs that do not cross the dotted line at y=1 represent significant differences relative to the control at α =0.05.

(B) Mel92.1 and Mel202 cell proliferation following transfection with Ctrl, GEP100#1, and GEP100#2 siRNAs as assessed by DNA content using CyQUANT and a fluorescence microplate reader. FU = Fluorescence units.

(C) Anchorage-independent colony growth of cells transfected as in panel B. The graph shows the percent DNA content relative to the control. Scale bar: 250 μm.

(D) Immunoblots of co-immunoprecipitated (Co-IP) oncogenic GNAQ and GEP100 in uveal melanoma cell extracts. IgG is negative control. To equalize signals, the amount of

immunoprecipitate loaded into the gel wells was reduced 19-fold for immunoblots probed with the GNAQ antibody. Data are represented as mean ± SD, n=3 experiments. One-way ANOVA, Dunnett's multiple comparisons test, ***$p < 0.001$.

See also Figures S4.

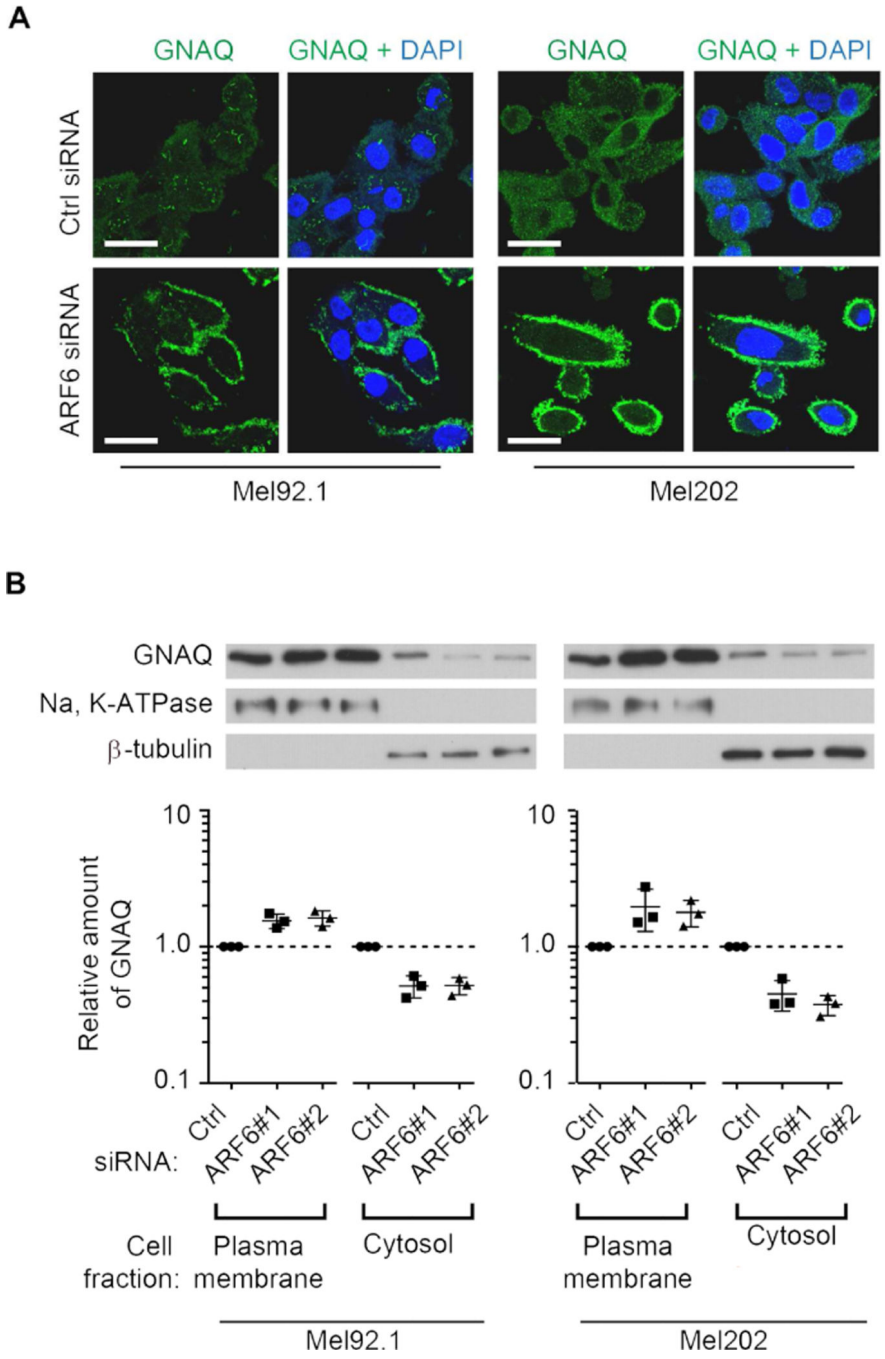

Figure 5. ARF6 controls GNAQ trafficking between the plasma membrane and cytoplasmic membranes/cytosol

(A) Immunocytofluorescent assays to assess GNAQ intracellular localization (green) following treatment of Mel92.1 and Mel202 cells with control (Ctrl) or ARF6 siRNA. Cells were counterstained with DAPI. Scale bar: 30 μm.

(B) Subcellular fractionation of GNAQ in Mel92.1 and Mel202 cells following treatment with two independent ARF6 siRNAs and Ctrl siRNA. Individual data points that have been normalized to the control are shown along with geometric means and 95% confidence

intervals (CIs). 95% CIs that do not cross the dotted line at y=1 represent significant differences relative to the control at α=0.05. n=3.
See also Figures S5.

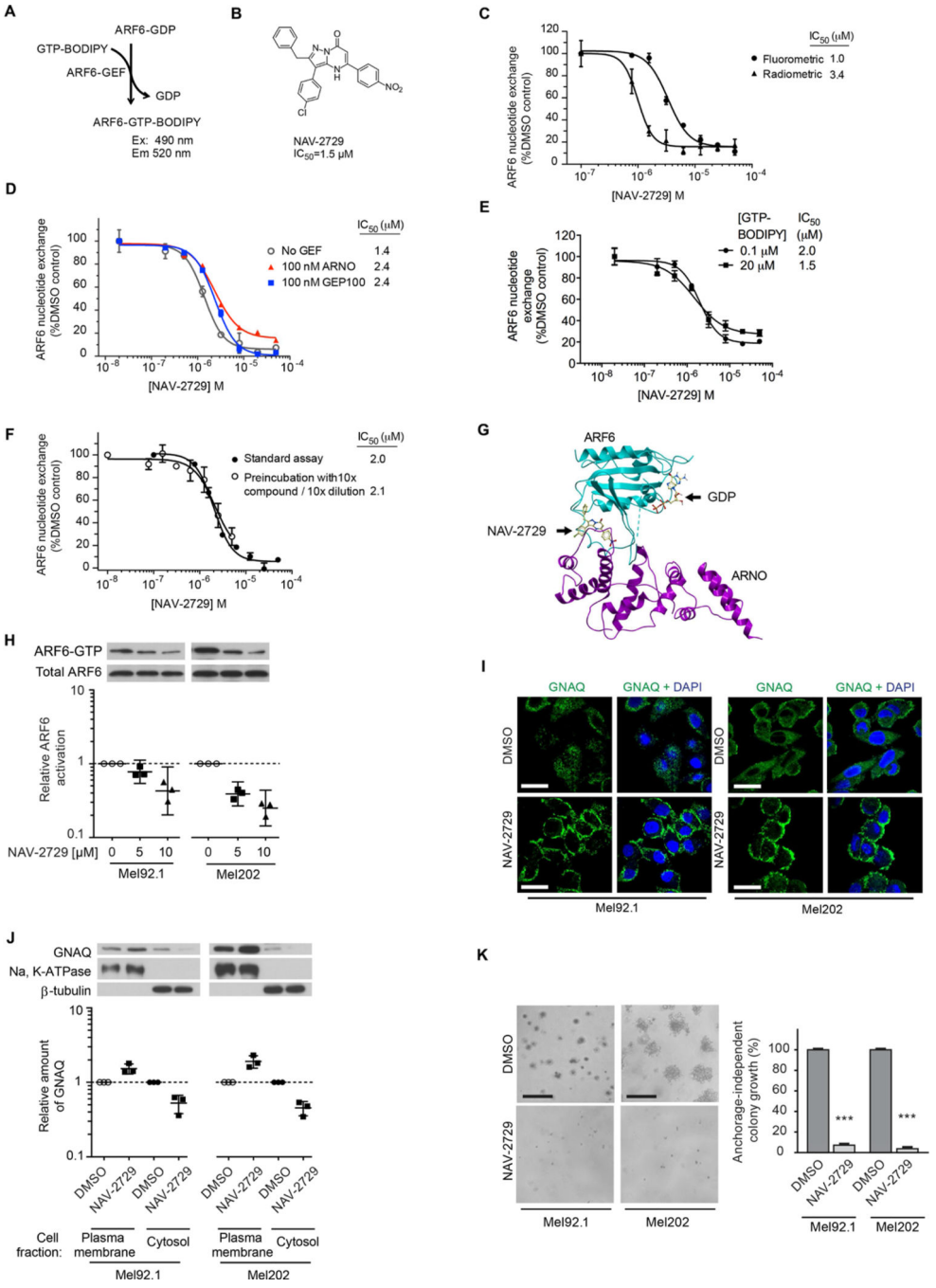

Figure 6. Discovery, confirmation, and assessment of NAV-2729

(A) Principle of high-throughput assay.

(B) Structure and average IC_{50} of NAV-2729.

(C and D) Evaluation of NAV-2729 inhibitory potency on fluorometric and radiometric nucleotide exchange assays (C) and on ARNO-mediated or GEP100-mediated ARF6 nucleotide exchange assays (D).

(E) Assay for the effect of GTP-BODIPY concentration on NAV-2729 inhibitory potency.

(F) Test for reversibility of NAV-2729 inhibition.

(G) Model of ARF6-ARNO complex showing where NAV-2729 interacts with the complex.
(H) Immunoblots of ARF-GTP pull-downs following treatment of Mel92.1 and Mel202 cells with NAV-2729 or vehicle (0).
(I) Immunocytofluorescent assays to assess GNAQ intracellular localization (green) in uveal melanoma cells following NAV-2729 or DMSO (vehicle) treatment.
(J) Subcellular fractionation of GNAQ in Mel92.1 and Mel202 cells treated with NAV-2729 or DMSO (vehicle).
(K) Anchorage-dependent colony growth in Mel92.1 and Mel202 cells treated with NAV-2729 or DMSO (vehicle). The graph shows the percent DNA content relative to the control. Data are represented as mean ± SD, n=3 experiments. Holm-Sidak multiple t test analysis, ***$p < 0.001$.
For panels H and J, individual data points have been normalized to DMSO (vehicle) and are shown along with geometric means and 95% confidence intervals (CIs). 95% CIs that do not cross the dotted line at y=1 represent significant differences relative to the control at $\alpha=0.05$. n=3.
See also Figure S6.

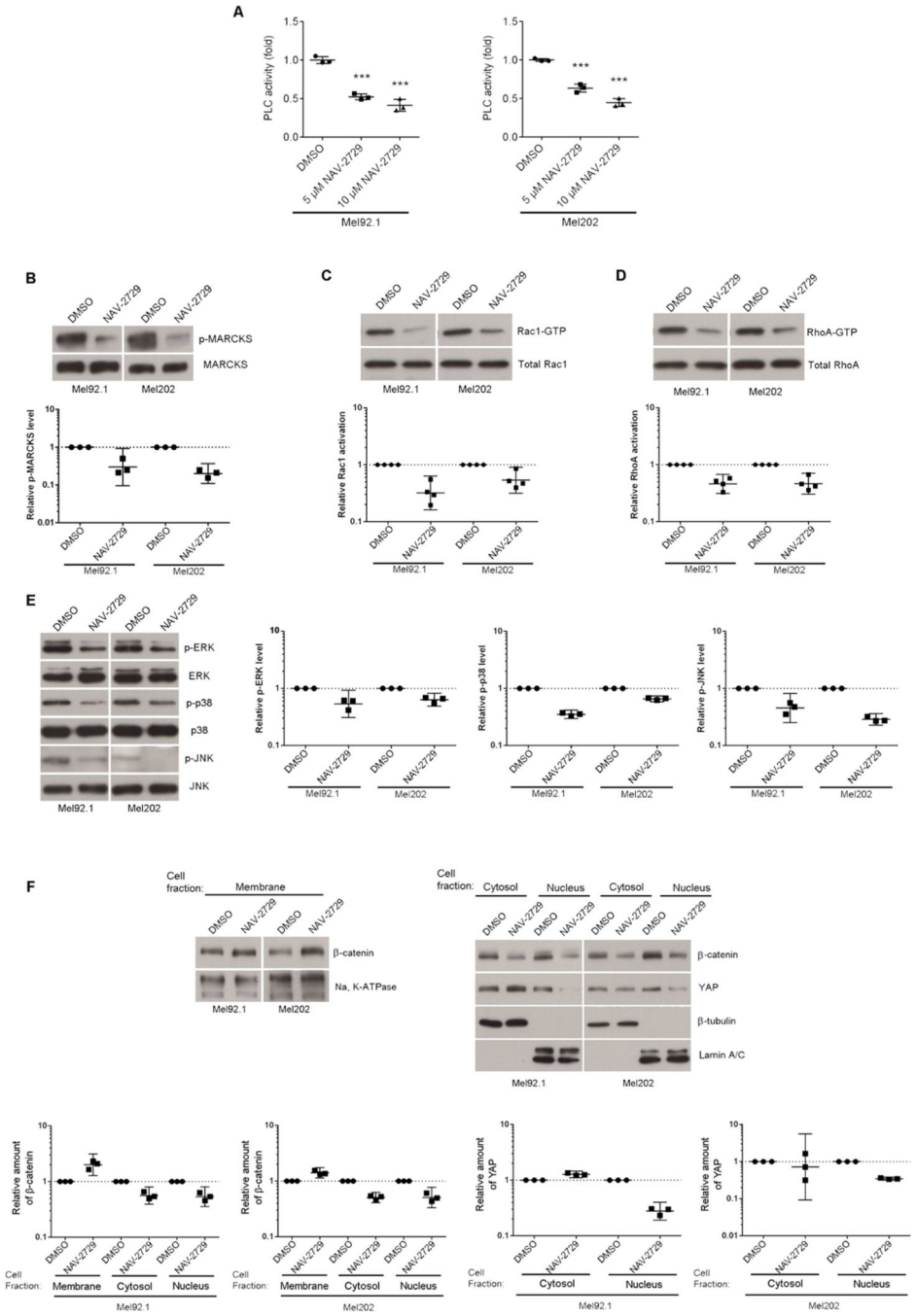

Figure 7. NAV-2729 inhibits all known signaling pathways downstream of oncogenic GNAQ in uveal melanoma cells

In each panel, Mel92.1 and Mel202 cells have been treated with either DMSO (vehicle) or 10 μM NAV-2729, unless otherwise indicated.

(A) Relative PLC activity.

(B) Relative activation, i.e., phosphorylation (p-) of MARCKS.

(C) Relative Rac1 activation (Rac1-GTP).

(D) Relative RhoA activation (RhoA-GTP).

(E) Relative activation (phosphorylation) of ERK, p38, and JNK.

(F) Intracellular localization of β-catenin and YAP by subcellular fractionation. n=3 or 4 experiments as indicated. A representative immunoblot is shown for each downstream marker. Each experiment is represented by a single data point that has been normalized to its DMSO (vehicle) control. Geometric means and 95% confidence intervals (CIs) are shown. 95% CIs that do not cross the dotted line at y=1 represent significant differences relative to the control at α=0.05.

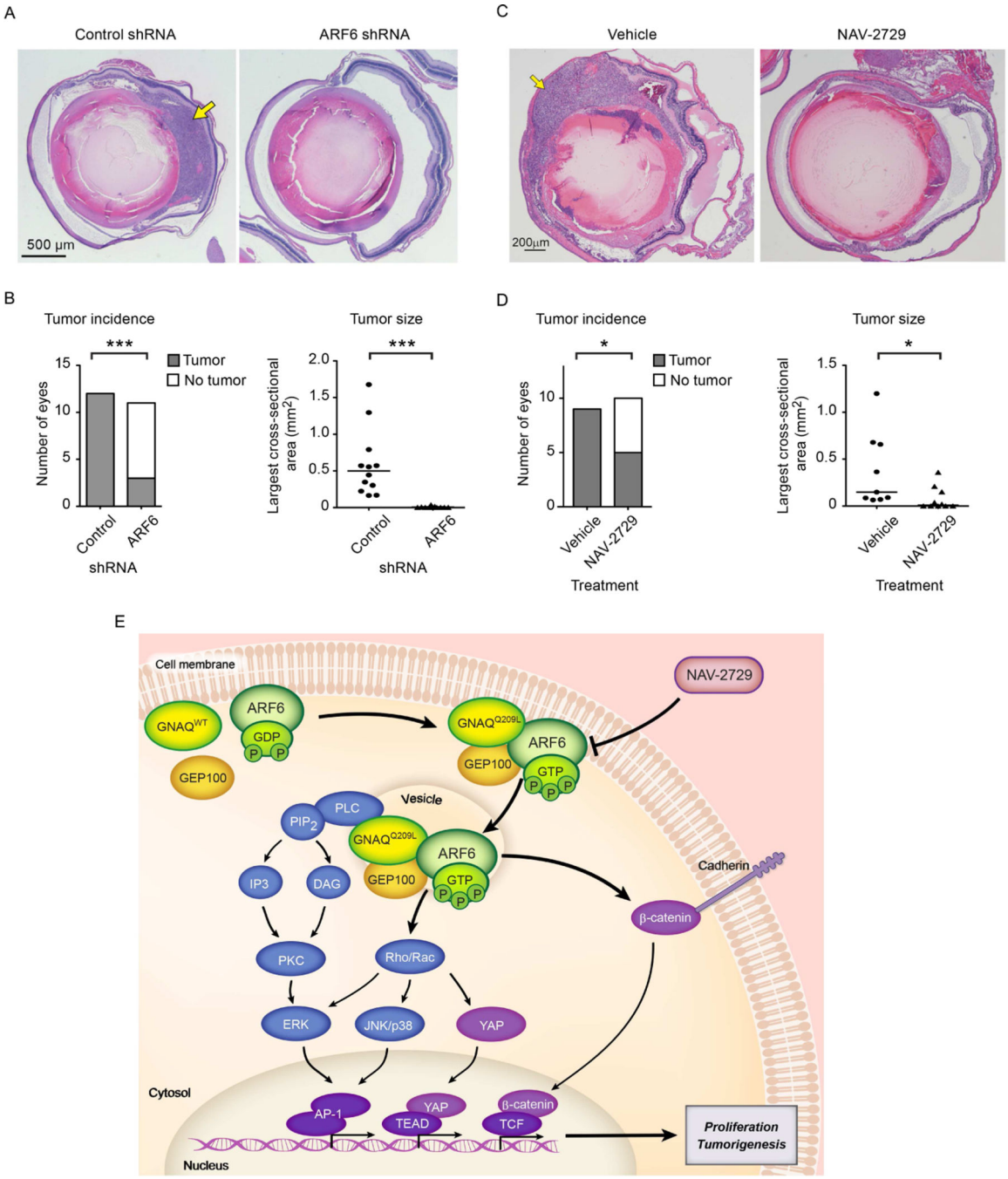

Figure 8. Silencing or pharmacological inhibition of ARF6 reduces uveal melanoma tumorigenesis *in vivo*

(A) Hematoxylin and eosin (H&E) stained sections from eyes engrafted with Mel202 cells expressing either control or ARF6 shRNAs. Scale bar: 500 μm.

(B and D) *Left*, number of eyes with and without a tumor (Fisher's exact test). *Right*, primary tumor size (median; Mann-Whitney U test). *p < 0.05, ***p < 0.001. n=11 and 12.

(C) H&E stained sections from eyes engrafted with Mel202 cells, followed by treatment of mice with either vehicle or NAV-2729 (daily IP injections at 30 mg/kg body weight). Scale

bar: 200 μm. Arrows in panels A and C point to clusters of uveal melanoma cells. n=9 and 10.

(E) Proposed oncogenic GNAQ/GEP100/ARF6 signaling pathway.

See also Figure S7 and Tables S1– S3.